

REPORT DOCUMENTATION PAGE

Form Approved
OMB No. 0704-0188

Public reporting burden for this collection of information is estimated to average 1 hour per response, including the time for reviewing instructions, searching existing data sources, gathering and maintaining the data needed, and completing and reviewing the collection of information. Send comments regarding this burden estimate or any other aspect of this collection of information, including suggestions for reducing this burden, to Washington Headquarters Services, Directorate for Information Operations and Reports, 1215 Jefferson Davis Highway, Suite 1204, Arlington, VA 22202-4302, and to the Office of Management and Budget, Paperwork Reduction Project (0704-0188), Washington, DC 20503.

1. AGENCY USE ONLY (Leave blank)	2. REPORT DATE	3. REPORT TYPE AND DATES COVERED MAJOR REPORT	
4. TITLE AND SUBTITLE "SPECIFIC AND SELECTIVE BIOSENSOR FOR SALMONELLA AND IT'S DETECTION IN THE ENVIRONMENT"			5. FUNDING NUMBERS
6. AUTHOR(S) CAPT OLSEN ERIC V			
7. PERFORMING ORGANIZATION NAME(S) AND ADDRESS(ES) AUBURN UNIVERSITY MAIN CAMPUS			8. PERFORMING ORGANIZATION REPORT NUMBER CI02-1256
9. SPONSORING/MONITORING AGENCY NAME(S) AND ADDRESS(ES) THE DEPARTMENT OF THE AIR FORCE AFIT/CIA, BLDG 125 2950 P STREET WPAFB OH 45433			10. SPONSORING/MONITORING AGENCY REPORT NUMBER
11. SUPPLEMENTARY NOTES			
12a. DISTRIBUTION AVAILABILITY STATEMENT Unlimited distribution In Accordance With AFI 35-205/AFIT Sup 1		12b. DISTRIBUTION CODE	
13. ABSTRACT (Maximum 200 words)			
DISTRIBUTION STATEMENT A Approved for Public Release Distribution Unlimited		20030825 029	
14. SUBJECT TERMS			15. NUMBER OF PAGES 35
			16. PRICE CODE
17. SECURITY CLASSIFICATION OF REPORT	18. SECURITY CLASSIFICATION OF THIS PAGE	19. SECURITY CLASSIFICATION OF ABSTRACT	20. LIMITATION OF ABSTRACT

THE VIEWS EXPRESSED IN THIS ARTICLE ARE THOSE OF
THE AUTHOR AND DO NOT REFLECT THE OFFICIAL
POLICY OR POSITION OF THE UNITED STATES AIR
FORCE, DEPARTMENT OF DEFENSE, OR THE U.S.
GOVERNMENT

Final copy: August 26, 2008

1 Specific and selective biosensor for *Salmonella* and its detection in the environment

2

3 E. V. Olsen^a, S.T. Pathirana^b, A.M. Samoylov^b, J.M. Barbaree^a, B.A. Chin^c, W.C. Neely^d, and V.
4 Vodyanoy^{b*}

⁵ *^aDepartment of Biological Sciences, Auburn University, Alabama 36849, USA*

⁶*Department of Anatomy, Physiology and Pharmacology, Auburn University, Alabama 36849,
7 USA*

^c*Material Research & Education Center, Auburn University, Alabama 36849, USA*

^dDepartment of Chemistry, Auburn University, Alabama 36849, USA

10

11 *Corresponding author. Tel.: +1-334-844-5405; fax:+1-334-844-5388.

12 *E-mail address:* vodyavi@vetmed.auburn.edu (V. Vodyanoy)

13 Complete correspondence address: Vitaly Vodyanoy, Department of Anatomy, Physiology and
14 Pharmacology, 109 Greene Hall, Auburn University, AL 36849, USA

15

* Corresponding author. Tel.: 1-334-844-5405; e-mail: vodyavi@vetmed.auburn.edu

1 **Abstract**

2 The specific and selective detection of *Salmonella typhymurium* based on the use of a
3 polyclonal antibody immobilized by the Langmuir-Blodgett method on the surface a quartz
4 crystal acoustic wave device was demonstrated in liquid samples. These biosensors were
5 selective to *Salmonella typhymurium* in the presence of large concentrations of *Escherichia coli*
6 O157:H7. They were also specific to *Salmonella typhymurium* since bacteria preincubated with
7 free antibody produced no signal. Dark-field and electron microscopy showed that two different
8 antibodies, polyvalent somatic O and flagellar H7, were immobilized on the sensor surface
9 producing two distinct attachments of bacteria at the liquid/solid interface. The somatic O
10 antibody exhibits a rigid, binding, while the flagellar H7 antibody forms a flexible connection
11 allowing a large degree of freedom. When the attachment of bacteria was rigid and strong, the
12 responses of the acoustic wave sensors correlated with changes in the mass of bacteria present at
13 the liquid-solid interface. In contrast, when attachment was flexible the sensor signals were
14 inversely proportional to the additional mass of bound bacteria. This difference is probably
15 determined by the interfacial viscoelasticity and by acoustic and electromagnetic coupling. The
16 signals of environmentally aged sensors with either predominately rigid or flexible positioning of
17 bacteria were correlated with changes in mass at the liquid-solid interface. Sensors with O or H
18 type of binding could be used for analytical purposes.

19

20 **Keywords:** Acoustic wave device; biosensor; Langmuir-Blodgett monolayer; antibody

21

1. Introduction

2 The thickness-shear-mode (TSM) acoustic wave sensor is proven to be an excellent
3 analytical tool for the study of specific molecular interactions at the solid-liquid interface (Bunde
4 et al., 1998, O'Sullivan and Guilbault, 1999, Cavicacute, et al., 1999, Ivnitski , et al., 1999,
5 Kaspar et al., 2000). Acoustic waves in TSM are excited by the application of a radio frequency
6 alternating voltage to the piezoelectric crystal. Changes in the resonance frequency are usually
7 attributed to the effect of the added mass due to the binding at the solid-liquid interface. Acoustic
8 wave sensors with immobilized biological recognition molecules (biosensors) were utilized for
9 the real-time study of the adsorption of biochemical macromolecules (Ghafouri and Thompson,
10 1999). Acoustic wave devices were shown to be quite specific immunosensors in complex
11 biological media containing cells and human serum (Dahint, et al., 1999). The theoretical model
12 of the responses of TSM resonators was proven experimentally under various loading conditions,
13 including an ideal mass layer (thin layers of gold and SiO_2), a semi-infinite fluid (glycerol in
14 water), and a viscoelastic layer exemplified by thin layers of oil (Martin et al., 1991, Bandey et
15 al., 1999). When TSM crystals were exposed to relatively large protein and polysaccharide
16 molecules, the responses obtained for those interactions were not correlated with change in mass
17 imposed at the liquid-solid interface (Ghafouri and Thompson, 1999). The authors ascribed this
18 phenomenon to viscoelastic and acoustic coupling at the interface. One could expect even more
19 complicated interfacial properties when the TSM sensor is exposed to much larger species, like
20 viruses and bacteria. Electromechanical forces created by live and moving organisms may
21 contribute to the apparent mass of the bacteria. Factors such as nutrition, growth, differentiation,
22 chemical signaling, and mutagenic exposure, are important in controlling the bacterial physical
23 state. The bacterial cell (e.g. *E. coli*), is about one million times heavier than a typical (150 kD)

1 antibody molecule (Neidhardt, 1987). Many bacteria are involved in various movements
2 controlled by flagella, Brownian motion, chemotaxis, swimming behavior, adaptation, and other
3 cell phenomena (Alberts et al., 1989). The ability to bind may also depend on fimbriae and
4 properties of single cells to associate and form colonies. The interaction of bacteria with the
5 biosensor may become dependent on environmental conditions.

6 The acoustic devices theory and biological applications were recently reviewed (Kaspar et
7 al., 2000, Cavicacute, et al., 1999, Ivnitski , et al., 1999).

8 In our previous work we demonstrated the feasibility of a biosensor based on Langmuir-
9 Blodgett monolayers of an antibody for the rapid and sensitive detection of *Salmonella*
10 *typhimurium* in liquid samples (Pathirana, et al., 2000). In the present work we investigated
11 specificity and selectivity of the biosensor under environmental conditions and after
12 environmental aging of the biosensors. Additionally, we studied the effects on the biosensor
13 signal of bacterial positioning at the liquid-surface interface.

14 **2. Materials and methods**

15 *2.1. Cultures.*

16 *Salmonella typhimurium* and *Escherichia coli* O157:H7 cultures from the Auburn
17 University culture collection were used in these experiments. Each culture was confirmed for
18 identity using traditional biochemical, cell morphology, and serologic tests. The cultures were
19 maintained on Trypticase agar (TSA) slants.

20 *2.2. Growth of cultures and dilutions.*

21 Each culture was streaked for isolation on TSA plates before inoculation of a fresh
22 culture to trypticase soy broth for overnight incubation at 37 °C in a shaking water bath

1 incubator. The cells were then washed by centrifugation (3500 rpm for 10 minutes) of the broth
2 and resuspension in 10 mL of sterile phosphate buffered saline (PBS) (pH 7.0) then repeating
3 centrifugation and resuspension in 2 mL PBS. Aseptic procedures were used throughout the
4 procedure. Serial dilutions were made with PBS. All tubes were shaken before each pipetting to
5 assure mixing before delivery.

6 *2.3. Colony forming unit (CFU) determinations.*

7 The number of viable cells in each dilution was determined by spread plating 0.1 mL of
8 each dilution onto duplicate plates of TSA, and incubating 48 hours before making a final count
9 of the CFU/ml and calculating the average CFU based on dilutions yielding 30-300
10 colonies/plate. The tubes with diluted cells were immediately placed on ice and delivered to
11 another laboratory for testing with the sensor.

12 *2.4. Antibodies.*

13 Antibodies used as capture antibodies on the membranes attached to the sensor were
14 obtained from Oxoid, Inc. (Ogdensburg, NY). For *S. typhimurium*, a polyvalent somatic O
15 antibody specific for most *Salmonella* serovars was employed. To capture *E. coli* O157:H7,
16 polyvalent H7 (flagellar) antibodies were used. In most cases, the same lot of antibody was used
17 throughout. Reactivity was checked against the target bacterium by a slide agglutination test.

18 *2.5. Procedures for examining the reactivity of antibodies.*

19 Three types of tests were employed to examine the reactivity of antibodies:
20 (1) a dot blot ELISA test using nitrocellulose or nylon filters with antigen fixed and subjected to
21 chromogenic anti-mouse (for monoclonal antibody) or anti-animal-based antibody conjugated
22 with enzyme assay; (2) kit tests for target organisms; and (3) agglutination tests.

1 2.6. *Monolayer techniques.*

2 2.6.1. *Surface Film Balance.*

3 Measurements of surface pressure were performed using a Langmuir-Blodgett film
4 balance KSV 2200 LB (KSV-Chemicals, Finland). This fully computerized system contains a
5 Wilhelmy-type surface balance (range 0-100 mN/m; sensitivity 0.05 mN/m), a Teflon trough
6 (45x15 cm²), a variable speed motor-driven Teflon barrier (0-200 mm/min), and a laminar flow
7 hood. The trough was mounted on a 200 kg marble table. Vibration control was provided by
8 interposing rubber shock absorbers, and by mounting the laminar flow hood on a separate bench.
9 Surface pressure was monitored by the use of a sandblasted platinum plate of 4 cm perimeter.
10 Temperature of the subphase was controlled (± 0.1 °C) by water circulation through a quartz
11 tube coil on the bottom of the trough. Temperature was measured by a thermistor located just
12 below the water interface. Surface pressure data were collected during slow, steady-state
13 compression of the monolayers

14 2.6.2. *Monolayer formation and deposition.*

15 *Phospholipid monolayers.* Phospholipid solutions were spread on the surface balance as
16 hexane solutions (1 mg/mL) containing 2% ethanol (Ito et al., 1989). The subphase used in the
17 experiments was a solution containing 55 mM KCl, 4 mM NaCl, 0.1 mM CaCl₂, 1 mM MgCl₂
18 and 2 mM 3-(N-morpholino)-propanesulfonic acid (MOPS) made with deionized double distilled
19 water (pH adjusted to 7.4 with KOH).

20 *Monolayers with immobilized antibodies.* The quartz crystals with gold electrodes for the
21 acoustic wave sensor were cleaned by treatment with 50 % (v/v) HNO₃ and were rinsed in
22 running distilled water until the acid was completely removed. The quartz crystals were then

1 dried and stored until use. The monolayer was formed on the air-liquid interface by allowing the
2 spreading solution to run down an inclined wettable planar surface that is partially submersed
3 into the subphase. One hundred and fifty μ L of the antiserum was spread on the subphase surface
4 by allowing it to flow down a wet glass plate that crossed the interface. The flow rate down the
5 plate was maintained at about 0.1 mL/min. After spreading, the glass plate was removed, and the
6 monolayer was allowed to equilibrate and stabilize for 10 minutes at $19 \pm 0.1^{\circ}\text{C}$. The
7 monolayer was then compressed at a rate of 30 mm/min and the vertical film deposition was
8 carried out with a vertical rate of 4.5 mm/min and at a constant surface pressure of 23 mN/m.
9 Seven monolayers of the *Salmonella* antibody film were transferred to the gold surface of the
10 quartz crystals in this manner. Monolayers containing antibodies were transferred at a constant
11 surface pressure onto the round ($d = 1''$) quartz crystals with gold electrodes for acoustic wave
12 device measurements, or onto standard microscope slides (test slides) for visual observations and
13 cell counting.

14 2.7. *Bacteria binding measurements.*

15 2.7.1 Acoustic Wave Device Measurements (AWD).

16 Measurements were carried out using Maxtek PM-740 or TM-400 monitors (Maxtek Inc,
17 Santa Fe Springs, CA) with a frequency resolution of 0.5 Hz at 5 MHz. The devices were
18 capable of working in both single and dual probe modes. Voltage output of the Maxtek device
19 was recorded and analyzed using a standard personal computer, data acquisition card and
20 software. The voltage output from the Maxtek device is directly related to the resonance
21 frequency of the quartz crystal sensor. Changes in the resonance frequency of the quartz crystal
22 sensor were used to monitor the binding of bacteria to the sensor surface. The observed changes

1 in the resonance frequency of the quartz crystal sensor during binding of bacteria is hypothesized
2 to be due both to viscoelastic changes of the LB film-bacteria-near surface fluid media and the
3 mass change associated with the binding of bacteria.

4 2.7.2. AWD quartz crystal sensors.

5 AT-cut planar quartz crystals with a 5 MHz nominal oscillating frequency were
6 purchased from Maxtek, Inc. Circular gold electrodes were deposited on both sides of the crystal
7 for the electrical connection to the oscillatory circuit.

8 2.7.3. Binding measurements.

9 The Quartz crystal microbalance was calibrated by the deposition of well-characterized
10 stearic acid monolayers. The sensor covered with the antibody film was positioned in the probe
11 arm of the instrument just before delivery of test solutions. Immediately after the recording was
12 started, 1000 μ L of the control solution was delivered with a pipette to the dry sensor surface and
13 the voltage was recorded for 4 - 8 minutes. Then the test solution was carefully removed with a
14 plastic pipette tip. After removal of the control solution a new recording was initiated and 1000
15 μ L of solution containing bacteria was added and the same measuring procedure was followed.
16 Temperature of the test solutions was controlled (± 0.1 $^{\circ}$ C). In order to examine the specificity
17 of bacteria binding by antibody immobilized in the sensor membrane, the sensor was exposed to
18 bacteria previously incubated with a solution of free antibody for the optimized contact time..
19 After all the solutions were tested, the sensor crystal was carefully removed and placed in
20 absolute ethanol and subsequently cleaned with concentrated nitric acid. All the equipment used
21 in the experiment was sterilized with ethanol. The data collected were stored and analyzed off
22 line.

1 2.8. *Dark-field microscopy.*

2 Optical observation and recording of bacteria binding were performed with an Olympus
3 microscope fitted with a 100-W mercury lamp illumination source, a polarizer, a Naessens dark-
4 field condenser (COSE Corp., Canada) and a 100 \times objective (oil, NA 1.4). The dark-field images
5 (Vodyanoy et al., 1994) were directed to a DEI-470T Optronics CCD Video Camera System
6 (Optronics Engineering, CA). The system provided real-time, direct-view optical images of high
7 resolution. The samples needed no freezing, dehydration, staining, shadowing, marking, or any
8 other manipulation. They were observed in the natural aqueous environment. A direct count of
9 bacteria was used to determine their concentrations in liquid samples. The count of bound
10 bacteria in the presence of a large concentrations of motile cells was used to estimate the surface
11 concentration of specific antibody.

12 2.9. *Environmental aging of sensors*

13 One hundred-forty eight *Salmonella* antibody sensors and 35 test slides were fabricated
14 by transferring 7 monolayers of *Salmonella* antibody serum to each of the quartz crystal
15 substrates and microscope slides using the LB technique. One hundred-forty samples were
16 divided into five sets: a control set, and sets with samples immersed in raw chicken exudate at
17 temperatures \sim 4°C, 11°C, 23°C and 33°C (Olsen, E. 2000). Each set of crystals was divided
18 into groups of 4 crystals and 1 test slide. The control group was tested immediately after
19 production. Each day for 7 days, 4 sensors and 1 test slide from other groups were removed from
20 the chicken exudate, rinsed and tested. The sensor was positioned in the holder of the acoustic
21 wave device and the output voltage of the balance was recorded for eight minutes after 1000 μ L
22 of the following solutions were applied in sequence: subphase solution, concentrated salmonella
23 suspension diluted 1/625, 1/125, 1/25, 1/5 and undiluted bacterial suspension. Eight initial (not-

1 aged) sensors were also tested as a control for interaction with *Salmonella* suspended in chicken
2 exudate and in exudate containing no *Salmonella*. The bacterial count was measured each day and
3 the concentrations were calculated accordingly. The concentration of bacteria ranged from 10^7 -
4 10^{10} cells/mL. The dose-response experiments were carried out at a temperature of 25^0C .

5

6 3. Results and discussion

7 *3.1. Rigid versus flexible positioning of bacteria onto the surface of acoustic wave sensor.*
8 When the somatic O antibody against *Salmonella* was employed the firm, whole body,
9 attachment of bacteria was confirmed by electron and dark field microscopy (Figure 1 and 2 A).
10 Electron micrographs show that bacterial binding in this case is characterized by the parallel
11 alignment of cells with visible filaments firmly attaching cells to the surface. The real time dark-
12 field recordings of live bacteria bound to the surface confirm this observation (Figure 2A). In
13 contrast, H7 flagellar antibodies provide a flexible attachment of cells to the sensor surface
14 allowing a large degree of freedom. The molecular machinery of a bacterium produces the
15 rotation of its flagella (Schuster and Khan, 1994). When a single flagellum is fixed to the surface
16 by an antibody, the molecular machinery of the bacterium generates a rotation of the whole cell.
17 This rotation can be videotaped; representative frames are shown in Figure 2 B. These figures
18 depicts nine consecutive positions of a rotating bacterium at intervals of about 100 ms. If
19 several flagella are bound to the surface, the video recording showed side-to-side oscillation of
20 cells (not shown). When sensors with somatic O antibodies against *Salmonella* were subjected to
21 environmental aging, dark-field observation of the sensors showed an increase in the surface
22 buildup of indigenous bacteria as the time of aging and the temperature were increased (Olsen,
23 2000). The buildup partially obstructed the antibodies on the sensor surface and the accessibility

1 of antibodies to *Salmonella* was decreased. Dark-field microscope observation showed that the
2 firm, whole body, binding of *Salmonella* was replaced with a loose attachment of bacteria with a
3 considerable degree of freedom as the time of the sensor aging and the temperature were
4 increased. Thus, the positioning of *Salmonella* at the sensor surface changed from rigid to
5 flexible as environmental aging occurred.

6

7 *3.2. Validation of mass measurements of monolayers.*

8 The deposition of increasing numbers of stearic acid monolayers onto the surface of an
9 acoustic wave crystal resulted in a linear increase of the mass (Figure 3). The deposition of a
10 single monolayer of the stearic acid on the crystal adds an additional mass of $2.5 \times 10^{-7} \text{ g/cm}^2$ (for
11 a 38 mNm^{-1} transfer surface pressure). This agrees well with the theoretical estimate based on the
12 molecular area of the stearic monolayer in the condensed state. At this state, the area per
13 molecule is $\sim 20 \text{ \AA}^2$ (for a single alkyl chain) (Davies and Rideal, 1963). The number of the
14 stearic acid molecules in a monolayer of 1 cm^2 is equal $1 \times 10^{16}/20 = 5 \times 10^{14}$. The mass of one
15 stearic acid molecule equals $284 \text{ g/mole}/6.023 \times 10^{23} \text{ molecules/mole} = 4.72 \times 10^{-22} \text{ g}$. The mass of
16 the single monolayer then is $1 \times 5 \times 10^{14} \times 4.72 \times 10^{-22} \text{ g} = 2.4 \times 10^{-7} \text{ g}$. This compares well with our
17 experimental value of $2.5 \times 10^{-7} \text{ g}$.

18

19 *3.3. Specificity and selectivity of bacterial binding*

20 Response curves obtained by exposing the sensor to buffer solutions containing different
21 concentrations of the bacteria were characterized by fast reaction, the attainment of a steady-
22 state, and very low non-specific binding (Pathirana, et al., 2000). In Figure 4, curve 1, the mean
23 values of the steady-state output sensor voltages are plotted as a function of bacteria

1 concentration from 10^2 to 10^{10} cells/mL. The dose response is linear over 5 decades of bacterial
2 concentration ($R>0.98$, $p<0.001$). The sensor sensitivity, measured as a slope of the linear
3 portion of the dose response, is 18 ± 5 mV per decade of *Salmonella* concentration, based on
4 experiments from 112 sensors. The interaction of *Salmonella typhimurium* with the antibody is
5 specific because the sensor does not respond to the bacteria preincubated with the antibody
6 (Figure 4, line 2). The estimated Hill coefficient (Pathirana, et al., 2000), n , was found to be
7 equal to 0.45 ± 0.02 indicating that 2 binding sites were needed to anchor one bacterial cell to the
8 sensor surface. Figure 5 shows the selectivity of the sensor. Line 1 represents the dose response
9 of the *Salmonella* biosensor to *Salmonella typhimurium* in the presence of 5.6×10^8 cells of *E.*
10 *coli*. Line 2 show the dose response of the *Salmonella* sensor to *E. coli* within the same range of
11 concentration with no *Salmonella* present. For any given concentration the sensor response for
12 *Salmonella* is greater than that for *E. coli*. A marked response difference for *Salmonella* over *E.*
13 *coli* is observed even when the number of *E. coli* exceeds the number of *Salmonella* by a factor
14 of 1000. The non-specific interactions of the sensor with *E. coli* were small and compare well
15 with those found using an antibody-immobilized QCM (Park et al., 2000, Si et al., 2001, Su et
16 al., 2001, Wong et al., 2002).

17 The sensors retain ~75% of their sensitivity (slope of V versus log concentration curve)
18 over a period of 32 days, and above 25 % after 64 days (Pathirana, et al., 2000).

19

20 3.4. Effects of rigid and flexible positioning of bacteria on the apparent mass measured by
21 acoustic wave device

22 We found that the bacterial microenvironment and location of the antigen on the surface
23 of a bacterium determines the value and the sign of the analytical signal generated by the

1 acoustic wave device. When molecules of antigen were located on the surface of the bacterial
2 envelope, thus providing firm and tight attachment to the sensor surface, the sensor output
3 voltage was found to be directly proportional to the logarithm concentration of free bacteria in
4 the liquid adjacent to the sensor surface (Figure 6A, upper line). The lower line of Figure 6A
5 indicates that bacteria with no antigen matching the sensor antibody, do not bind to the sensor
6 surface. In contrast, when the antibody was against the antigen located in the bacterial flagellum,
7 the attachment allows a great degree of freedom (rotation and oscillation) so that the output
8 signal of the sensor in was inversely proportional to the logarithm of free bacteria in solution
9 (Figure 6B, lower line). Again, bacteria with no matching antigen did not bind to the sensor
10 surface (Figure 6B, upper line). The decrease in voltage output of the sensor corresponds to an
11 increase in the resonance frequency of the sensor and hence an “apparent decrease” in effective
12 mass of bacteria attached to the surface. When sensors with somatic O antibodies against
13 *Salmonella* were subjected to environmental aging, the type of attachment of bound bacteria was
14 found to depend on the time of exposure. The flexible positioning of bacteria on the sensor
15 surface replaced the rigid one as time increased. With rigid positioning of bacteria, the dose
16 response plots were as shown in Figure 6A (upper line). When the flexible positioning of
17 bacteria became dominant, and mobility of the bound cells increased, the dose response signal
18 became similar to that of the flagella bound cells shown in Figure 6B (lower line). Figure 7
19 shows that the responses of the somatic antibody type *Salmonella* sensor aged for six days at the
20 temperature 4 °C decreased as the *Salmonella* concentration increased. When bacteria were
21 bound with the mixed positioning, the dose response signal depended on the relative contribution
22 of cells with predominantly rigid or predominantly flexible attachment. Control experiments

1 with fresh (not aged) *Salmonella* sensors measuring *Salmonella* in the chicken exudate and in
2 exudate alone demonstrated low non-specific adsorption (data not shown).

3 If we define the sensitivity of the biosensor as the slope of the linear portion of the dose
4 response (signal ΔV in mV per decade of *Salmonella* concentration) then the sensitivity of the
5 sensors is expected to be positive or negative value for the predominantly rigid or flexible
6 positioning, respectively. The experimental dose response data for environmentally challenged
7 sensors were fitted by a linear regression analysis to a line $\Delta V = A + S \times \log(C)$, the slope of the
8 line (sensitivity), S, and the regression coefficient, R, were calculated for each sensor. We found
9 the regression coefficient, R, ranged from about + 0.98 (direct linear correlation), through zero
10 (no linear correlation) to -0.98 (inverse linear correlation) for positive, zero, and negative
11 sensitivities, respectively (Appendix). Figure 8 shows the experimental regression coefficient as
12 the function of sensitivity of *Salmonella* sensors. The majority of the aged sensor sensitivity
13 values for measurements carried out between 4°C and 33°C fell between -30 and +30
14 mV/decade. It is clear that from these results that the acoustic wave sensor has acceptable
15 analytical value for detecting bacteria only if positioning of bacteria on the sensor surface is
16 either predominantly rigid or predominantly flexible. In the mixed cases the sensitivity and
17 correlation coefficient for dose response signals are not favorable for the effective detection of
18 bacteria. The practical resolution for this phenomenon would be the ensuring of adequate
19 bacterial binding by using antibodies (or other recognition molecules) with high affinity and
20 multiple binding valences. The antibodies should be specific for either somatic or flagella
21 proteins and they must not to be used simultaneously on the same acoustic wave sensor.

22

1 The observed changes of apparent mass as a function of bacterial concentration are
2 hypothesized to be due both to viscoelastic changes of the LB film-bacteria near surface fluid
3 media and the mass change associated with binding of the bacteria. The most peculiar results
4 show that at certain controlled conditions there is an appearance of a negative apparent mass, i.e.
5 with increasing bacterial concentration there can be a dose dependent decrease of the apparent
6 mass. The exact mechanism producing the negative apparent mass is not known. However, this
7 effect may be due to different physical, chemical, and biological mechanisms. These include
8 electrochemical interaction between cells and the diffusion layer of ions on the sensor/liquid
9 interface, high frequency electrophoretic driving force, the viscoelasticity of bacterial cells,
10 physiological effects including electromechanical forces created by the live, moving organisms.

11
12 There are two very different positions where bacterial antigens may bind with antibodies
13 immobilized on sensor surfaces: O somatic antigens, derived from the outer membrane of
14 bacteria, and H antigens, derived from flagella proteins. Figure 9 shows these different binding
15 sites and at least 3 different ways in which the bacterial cells may bind to the sensor surface.
16 Viscoelastic properties of the bacterial layer attached to the surface are anticipated to be different
17 depending on the mechanism of binding: somatic or flagellar. For the three cases shown in
18 Figure 9 the viscous shear and viscous drag forces of the attached bacteria are very different. It is
19 clear that bacteria at the rigid and flexible positioning (Figure 9, A and B) take different roles in
20 the oscillation of the whole system. When the binding is rigid, bacteria oscillate in unison with
21 the crystal and therefore contribute to the effective oscillating mass of the system. This is shown
22 by the increase of the apparent mass when concentration of bacteria is increased. In the case of
23 flexible attachment, the oscillation of the bacteria may be not in phase with the oscillation of the

1 crystal and thus can cause a decrease in the apparent mass when concentration of the bacteria is
2 increased. Additionally, the electrically charged bacterium on the surface of an acoustic wave
3 crystal is not only engaged in the mechanical oscillations of the crystal but also directly interacts
4 with the electric field driving the sensor crystal. This field drives the piezoelectric quartz crystal
5 and at the same time creates an electrophoretic force applied to the electrically charged bacteria.
6 The piezoelectric and electrophoretic forces can be of different values and directions, depending
7 on positioning of bacteria by O antigen (firm positioning, Figure 9 A) or H antigen (flexible
8 attachment, Figure 9 B) and their combination can contribute to the change of the apparent mass
9 of the bacteria as measured by the acoustic device.

10

11 4. Conclusions

12 The results of this work demonstrate the high specificity and selectivity of biosensors based
13 on LB monolayers of an antibody deposited on a piezoelectric crystal for rapid detection of
14 bacteria in liquid samples. A marked selectivity for *Salmonella* over *E. coli* for *Salmonella* was
15 observed even when the number of *E. coli* exceeded the number of *Salmonella* by a factor of
16 1000. Results also indicate the importance of positioning of bacteria on the sensor surface. When
17 attachment of bacteria is rigid and strong the responses obtained for the interaction of the
18 bacteria with somatic O-type antibodies on the surfaces of acoustic wave sensors correlated
19 directly with changes in mass imposed at the liquid-solid interface. In contrast, when attachment
20 is flexible, as observed for bacteria attached by flagella to H-type antibodies, the sensor signals
21 were inversely proportional to additional mass, and are probably determined by interfacial
22 viscoelasticity and acoustic and electromagnetic coupling. The responses of environmentally
23 aged sensors with the predominantly rigid or flexible positioning of bacteria were correlated with

1 changes in mass at the liquid-solid interface. Sensors with O or H type of binding could be used
2 for analytical purposes.

3 **Appendix**

4 **Simplified analysis of the thickness-share mode acoustic resonator.**

5 The acoustic wave resonator (Figure10 A) admittance ($Y(\omega)$) can be expressed by the
6 equation:

7 $Y(\omega) = j\omega C_0 + 1/Z_m,$ (1)

8 Where ω is the angular frequency

9 $\omega = 2\pi f,$ (2)

10 C_0 is the static capacitance of the quartz sensor (we neglect any parasitic capacitance), and Z_m is
11 the motional impedance for the unloaded resonator (Martin, et al., 1991).

12 $Z_m = R + j\omega L + 1/j\omega C,$ (3)

13 where R , L , and C are the resistance, the inductance and capacitance of the motional arm in
14 parallel with the capacitance C_0 . The series resonant frequency f can be determined as

15 $f = 1/2\pi(LC)^{1/2}$ (4).

16 When the resonator is loaded with solutions the resonant frequency changes due to small changes
17 of parameters L and C . The differential of resonant frequency, df , can be calculated as following:

18 $df = (\partial f / \partial L) dL + (\partial f / \partial C) dC$ (5),

19 where partial derivatives $\partial f / \partial L$ and $\partial f / \partial C$ can be calculated from the Eq. 4:

20 $\partial f / \partial L = - (f/2)/L$ (6)

21 $\partial f / \partial C = - (f/2)/C$ (7).

1 Substituting partial derivatives with Eqs (6) and (7), and replacing the differentials df , dL , and
2 dC with small changes of the values, we have:
3 $\Delta f/f = -1/2 \times (\Delta L/L + \Delta C/C)$ (8).
4 The Eq (8) fully agrees with Eq (27) of Martin, et al., 1991 if we consider that $\Delta C/C=0$. If
5 binding bacteria increases the effective mass of the resonator then the serial inductance (L)
6 representing a mass in the equivalent-circuit model, should increase with the increase of bacteria
7 concentration. On the other hand, the binding of the bacteria increases the effective thickness of
8 the resonator and, consequently, decreases the equivalent capacitance (C) of the circuit. The
9 firmly attached dense layer of bacteria creates a small increase of the thickness and the increase
10 in thickness is proportional to the increase in mass. However, bacteria attached by flagella can be
11 separated from the surface as far away as 5-7 microns. In this case, the increase of the effective
12 thickness of the bound layer is not proportional to the mass of bacteria because they occupy only
13 a fraction of the layer. The electrically charged layer of bacteria spatially separated from the
14 sensor surface can create a charge distribution, which is equivalent to the serial capacitor
15 connected to the equivalent capacitor of the crystal. We can speculate, further, that relative
16 changes of the inductance and capacitance are linear functions of the bacterial concentration (C):

$$17 \Delta L/L = \alpha \log(C) \quad (10)$$

$$18 \Delta C/C = -\beta \log(C) \quad (11),$$

19 where coefficients α and β are independent of bacteria concentration.

20 From Eqs (9-11) we have:

$$21 \Delta f/f = -1/2 \times \alpha(1-\beta/\alpha)\log(C). \quad (12).$$

22 The output voltage (V) of the Maxtek PM740 acoustic wave device is inversely related to
23 frequency f . So, we can replace $\Delta f/f$ with $-\Delta V/V$ in Eq. (12):

1 $\Delta V/V = 1/2 \times \alpha(1-\beta/\alpha)\log(C)$. (13).

2 Equation (13) indicates, that if the relative increase of the effective thickness is small compared

3 to increase of the effective mass ($\alpha > \beta$), then the relative change of the voltage ($\Delta V/V$) is directly

4 proportional to the logarithm of bacteria concentration (Figure10B, line $\alpha > \beta$). If the opposite is

5 true, and $\alpha < \beta$, then $\Delta V/V$ is inversely related to the concentration of bacteria (Figure10 B, line

6 $\alpha < \beta$). If $\alpha = \beta$ then $\Delta V/V$ does not depend on the bacteria concentration (Figure10B, line $\alpha = \beta$):

7 $\Delta V/V \sim 1/2 \times \alpha \log(C)$, if $\alpha > \beta$ (14);

8 $\Delta V/V \approx 0$, $\alpha \approx \beta$; (15)

9 $\Delta V/V \sim -1/2 \times \beta \log(C)$, if $\alpha < \beta$ (16).

10 When experimental dose response data are fitted by a linear regression analysis to a line

11 $\Delta V/V = A + B \log(C)$, the slope of the line (sensitivity), B, and the regression coefficient, R, are

12 calculated for each sensor. When $\alpha > \beta$ a good positive correlation with a large slope (sensitivity)

13 is also is expected to be confirmed by a high regression coefficient ($R \approx 1$). If $\alpha < \beta$, the regression

14 coefficient at a large negative slope tends to approach a large negative value ($R \approx -1$). At

15 conditions, when $\alpha \approx \beta$, $R \approx 0$. Thus the regression coefficient can be a function of the slope and

16 can vary from -1 to $+1$, for different sensors with an inverse and direct concentration

17 dependence, respectively. (Figure10C).

18

19 **Acknowledgements**

20 We thank Randy O. Boddie for technical assistance. This work was supported partially

21 by grants from USDA 99-34394-7546 and DARPA MDA972-00-1-0011.

22

1 **References**

2 Alberts, B., Bray, D., Lewis, J., Raff, M., Roberts, K., Watson, J.D. 1989. Molecular biology of cell.
3 Garland, NY.

4 Bandey, H.L., Martin, S.J., Cernosek, R.W., Hillman, A.R., 1999. Modeling the responses of
5 thickness-shear mode resonators under various loading conditions. *Anal. Chem.* 71: 2205-
6 2214.

7 Bunde, R.L., Jarvi, E.J., Jeffrey J. Rosentreter, J.J., 1998. Piezoelectric quartz crystal biosensors.
8 *Talanta* 46, 1223-1236.

9 Caviacute; B.A., Hayward, G.L., Thompson, M. 1999. Acoustic waves and the study of
10 biochemical macromolecules and cells at the sensor-liquid interface *The Analyst*, 124, 1405-
11 1420.

12 Dahint, R., Bender, F.; Morhard, 1999. Operation of acoustic plate mode immuno sensors in
13 complex biological media. *Anal. Chem.* , 71, 3150-3156.

14 Davies, L.T., Rideal, E.K. 1963. *Interfacial Phenomena*. New York: Academic Press.

15 Ghafouri, S., Thompson, M., 1999. Interfacial properties of biotin conjugate-avidin complexes
16 studied by acoustic wave sensor. *Langmuir*, 15, 564-572.

17 Ivnitski, D., Abdel-Hamid, I., Atanasov, P., Wilkins, E. 1999. Biosensors for detection of
18 pathogenic bacteria. *Biosensors & Bioelectronics* 14, 599-624.

19 Kaspar, M., Stadler, H., Weiss, T., Ziegler, C., 2000. Thickness shear mode resonators ("mass-
20 sensitive devices") in bioanalysis, *Fresenius' J. Anal. Chem.*, 366, 602-610

21 Martin, S.J., Granstaff, V.E, Frye, G.C. 1991. Characterization of quartz crystal microbalance
22 with simultaneous mass and liquid loading. *Anal. Chem.* 63, 2272-2281.

23 Neidhardt, F.C. 1987. Chemical composition of *E. coli*. In: *Escherichia coli and Salmonella*.

1 Neidhardt, F.C. (Ed.) American Soc. For Microbiology, Washington, pp. 3-6.

2 O'Sullivan, C.K., Guilbault, G.G., 1999. Commercial quartz crystal microbalances – theory and
3 applications. *Biosensors & Bioelectron.* 14, 663–670.

4 Olsen, E.V. 1994. Functional durability of a quartz crystal microbalance sensor for the rapid
5 detection of *Salmonella* in liquids from poultry packaging. MS Thesis, Auburn University,
6 Alabama, USA.

7 Park, I-S., Ki, W-Y., Namsoo Kim, N. 2000, Operational characteristics of an antibody-
8 immobilized QCM system detecting *Salmonella* spp. *Biosensors & Bioelectronics* 15, 167–
9 172.

10 Pathirana, S.T., Barbaree, J., Chin, B.A., Hartell, M.G., Neely, W.C., and Vodyanoy V. 2000.
11 Rapid and sensitive biosensor for *Salmonella*. *Biosensors & Bioelectronics*, 15, 135-141.

12 Schuster, C.S., Khan, S. 1994. The bacterial flagellar motor, *Annu. Rev. Biophys. Biomol.*
13 *Struct.* 23, 509– 539.

14 Si, S., Li, X., Fung, Y., Zhu D. 2001. Rapid detection of *Salmonella enteritidis* by piezoelectric
15 immunosensor. *Microchemical J.* 68, 21-27.

16 Su, X., Low, S., Kwang, J., Chew, V.H.T., Li, S.Y. 2001. Piezoelectric quartz crystal based
17 veterinary diagnosis for *Salmonella enteritidis* infection in chicken and egg *Sensors and*
18 *Actuators B: Chemical*, 75, 29-35.

19 Vodyanoy, V. , S. Pathirana, and W.C. Neely. 1994. Stearic acid assisted complexation of K⁺ by
20 valinomycin in monolayers. *Langmuir*, 10, 1354-1357.

21 Wong, Y. Y., Ng, S.P., Ng, M.H., Si, S.H., Yao, S.Z., Fung, Y.S. 2002. Immunosensor for the
22 differentiation and detection of *Salmonella* species based on a quartz crystal microbalance.
23 *Biosensors & Bioelectronics*, 17, 676-684.

1

2

3

1 **Figure legends**

2

3 Figure 1. Scanning electron microscope image of the biosensor surface after exposure to
4 *Salmonella typhimurium* (arrow). The bacteria were attached to the O-type somatic antibody
5 at the rough surface unpolished crystal covered with gold. The image exhibits the rigid
6 attachment of bacteria. Some filaments holding bacteria at the surface are visible.
7 Magnification, $\times 5,000$; bar = $5\mu\text{m}$.

8 Figure 2. Dark-field microscope images of bacteria at the surface of the acoustic wave crystal.
9 The images represent time lapse frames from continuous real time video recordings. A. The
10 rigid attachment of *Salmonella* to the sensor surface in PBS by somatic O-type antibody.
11 The attached bacteria do not move. B. The flexible attachment of bacteria with the flagellar
12 H-type antibody allows oscillation and rotation of cells at the crystal surface. Photographs
13 depict rotation of bacterium attached to the antibody by flagellum. Arrows show nine
14 consecutive positions of the rotated bacterium taken at the interval of about 100 ms.

15 Figure 3. Figure 1. Validation of measuring mass of bound monolayers by acoustic wave sensor.
16 The experimental thickness of multilayer is a linear function of the number of stearic acid
17 monolayers transferred to the sensor surface. The labels “wet multilayer” and “dry
18 multilayers” indicate sensors submerged in buffer solution and dry sensor, respectively.
19 Points show experimental data \pm SD, while lines represent linear fit ($R=0.921$, $P<0.02$;
20 $R=0.998$, $P<0.0001$, respectively).

21 Figure 4. Specificity of *Salmonella* sensor. Curve 1 represents the mean values of steady-state
22 sensor voltages as a function of *Salmonella typhimurium* concentrations from 10^2 to 10^{10}
23 cells/mL. The smooth curve is the sigmoid fit to the experimental data ($\text{Chisqr} = 5.9 \times 10^{-5}$).

1 Line 2 shows the dose responses of the sensor exposed to *Salmonella typhimurium*
2 suspensions incubated with *Salmonella* antibodies prior to the exposure. 1.2×10^9 cells were
3 incubated with *Salmonella* antibodies (~200 μ g) in 1 mL of PBS for 3 h 40 min. The straight
4 line is the linear least squares fit to the data ($R=-0.76$, slope= -9.0×10^{-5} v/decade).
5 Experimental data points were obtained by averaging about 200 data points of each steady-
6 state level of response curves; bars are S.D.

7 Figure 5. Selectivity of *Salmonella* sensor. Curve 1 represents the mean values of steady-state
8 output sensor voltages as a function of *Salmonella typhimurium* concentrations from
9 1.8×10^6 to 10^9 cells/mL in the presence of 5.6×10^6 cells/mL of *E. coli* O157:H7. The line is
10 the linear fit to the experimental data ($R=0.97$). Line 2 shows the dose responses of the
11 sensor exposed to *E. coli* O157:H7. The straight line is the linear least squares fit to the data
12 ($R=-0.71$). The voltage output was scaled up by a factor 5.

13 Figure 6. Dose responses for rigid and flexible positioning of bacteria. A. The curve labeled
14 “*Salmonella*” represents *Salmonella* dose responses of the sensor with the somatic O-type
15 *Salmonella* antibodies. The line labeled “*E. coli*” represents *E. coli* dose responses of the
16 sensor with the somatic O-type *Salmonella* antibodies. B. The line labeled “*Salmonella*”
17 represents *Salmonella* dose responses of the sensor with the flagellar H-type *E. coli*
18 antibodies. The curve labeled “*E. coli*” represents *E. coli* dose responses of the sensor with
19 the flagellar H-type *E. coli* antibodies. Curves represent the sigmoid fit to experimental
20 data. The straight lines obtained by the linear least square fit; bars are S.D.

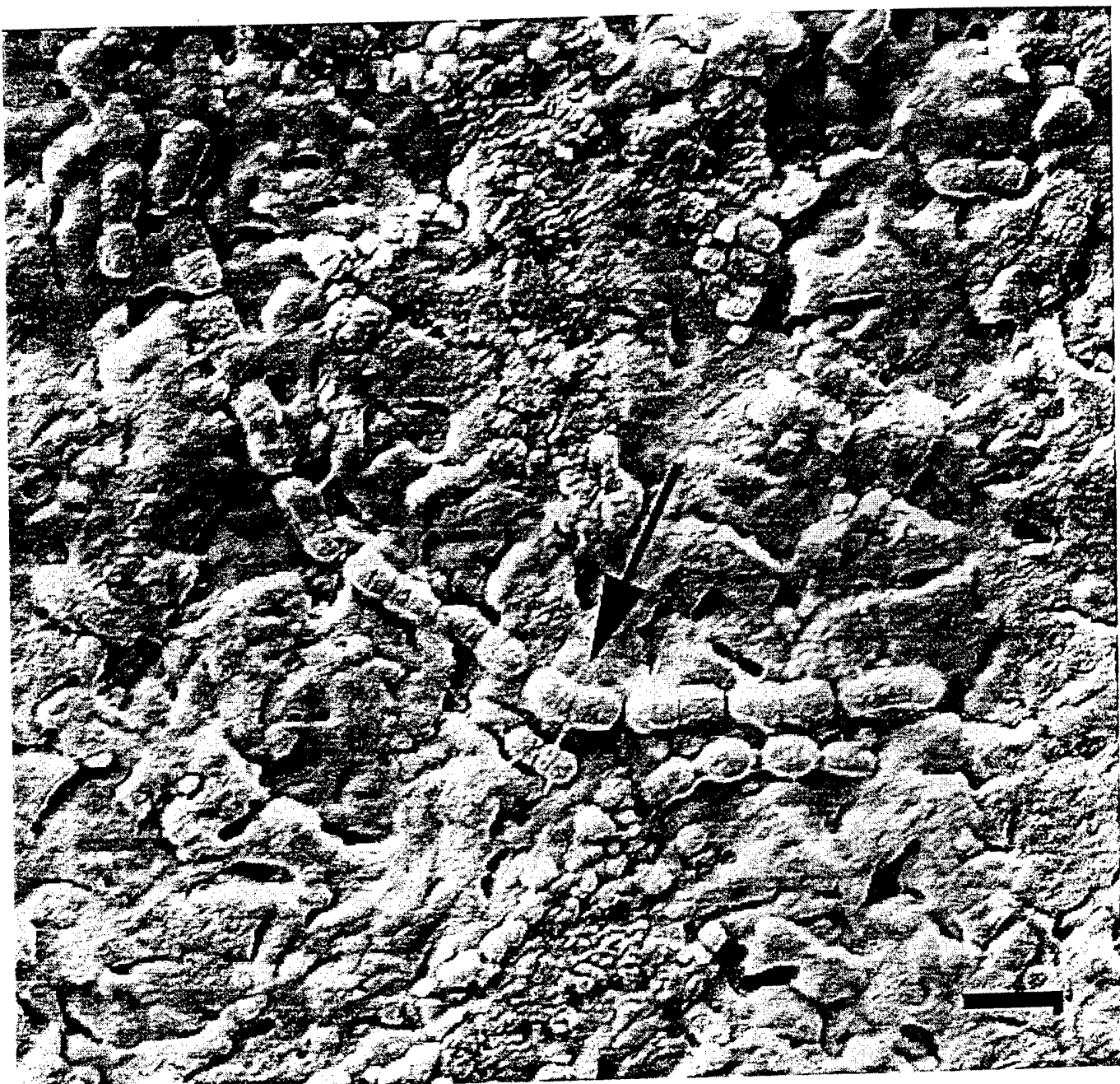
21 Figure 7. Dose responses of the sensor with the somatic O-type *Salmonella* antibodies to
22 *Salmonella*. The sensor was tested after it was environmentally aged for 6 days at 4°C.

1 Figure 8. The experimental regression coefficient as the function of sensitivity of *Salmonella*
2 sensors with the somatic O-type antibody for environmentally aged sensors. The linear
3 portions of dose response signals were fitted by linear regression. The regression
4 coefficients (R) were plotted against the slopes (sensitivity, mV/decade) for sensors aged at
5 temperatures indicated in the label. The line is the sigmoid fit, while the points are
6 experimental data.

7 Figure 9. Different positioning of bacteria at the surface of biosensor. A. The rigid attachment of
8 bacteria by the somatic O-type antibodies. The bacteria moves in unison with the crystal.
9 The electrophoretic force (F_e) applied to the electric charges of bacterium ("--") is aligned
10 with the cell body. The piezoelectric force F_p causes the particle displacement at the surface
11 of TSM sensor crystal. B. The flexible attachment of bacteria by the flagellar H-type
12 antibodies. The bacteria have a high degree of freedom and the displacements of crystal
13 particles may be not in phase with the displacements of the bacteria. C. In the aged sensors a
14 biofilm covers certain antibody binding sites and guards against polyvalent attachment of
15 bacteria. As result, the bound bacteria have more degree of freedom than the bacteria with
16 the firm attachment.

17 Figure 10. Simplified electrical model of biosensor. A. Equivalent circuit of TSM resonator
18 (Martin et al., 1991): a capacitance C_0 in parallel with resistance R , inductance L , and
19 functional capacitance C . B. Dose response dependence described by Eq. 13. C. Plot of the
20 correlation coefficient as the function of the sensitivity.

21



1
2
3
4
Figure 1

1
2
3
4
5
6
7
8
9
10
11
12
13
14
15
16
17
18
19
20
21
22
23
24
25

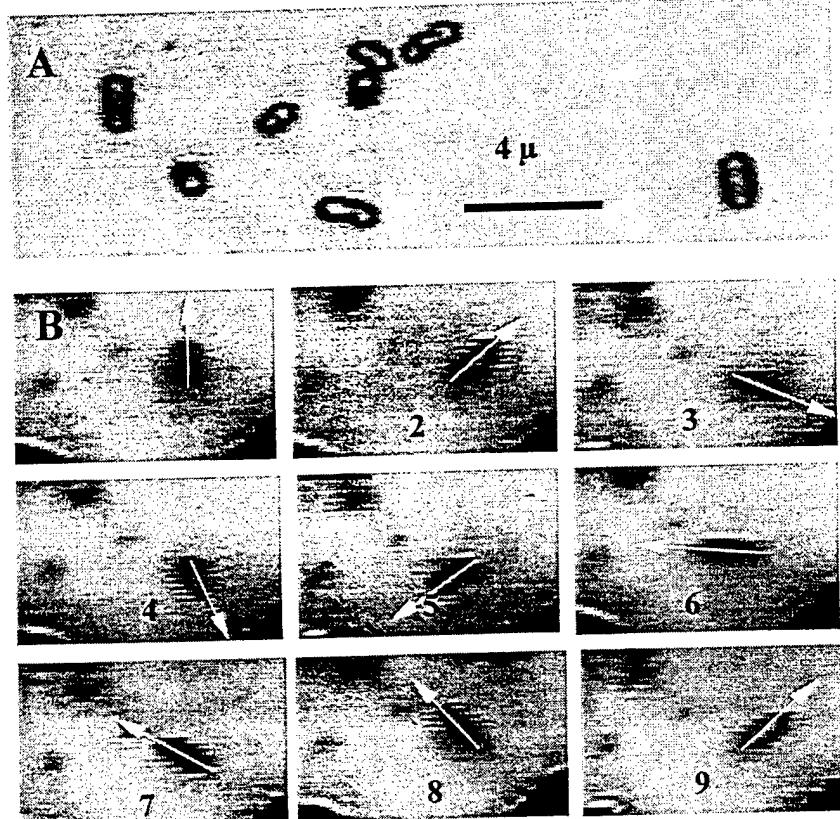


Figure 2.

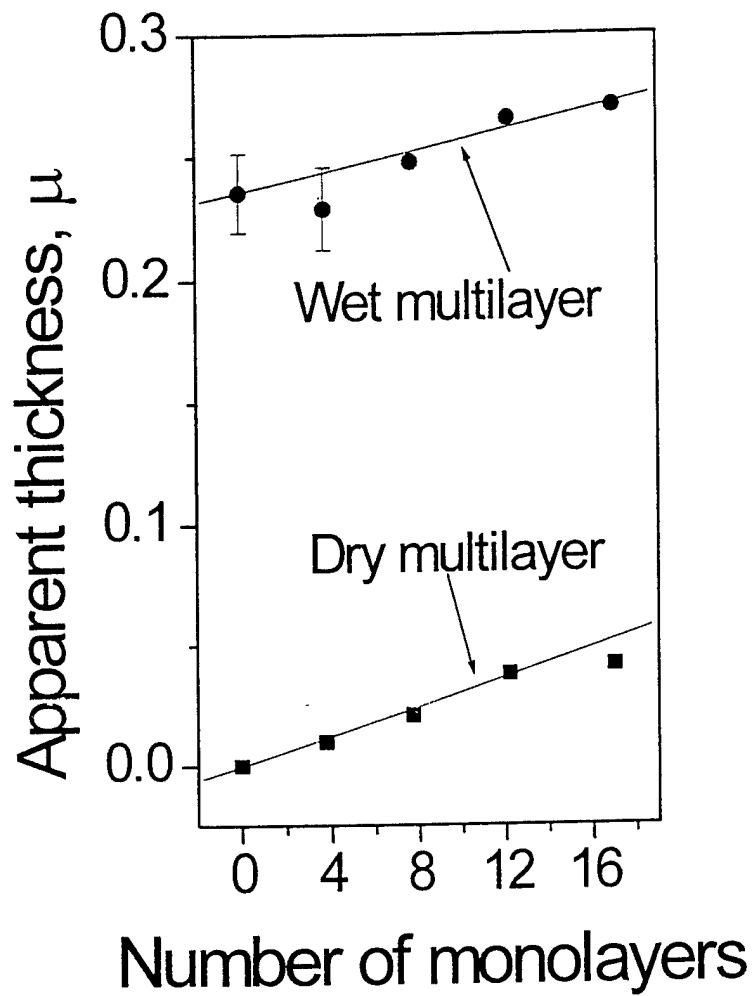
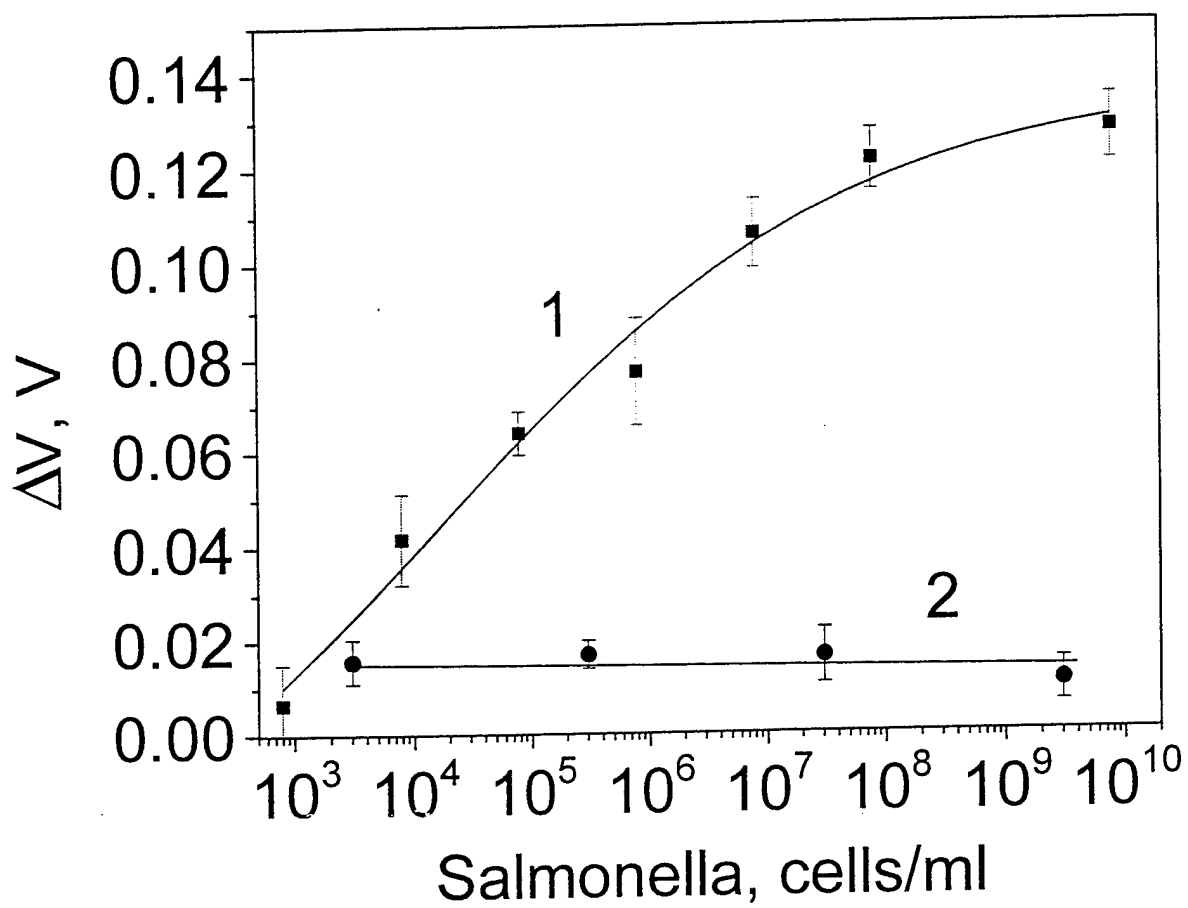
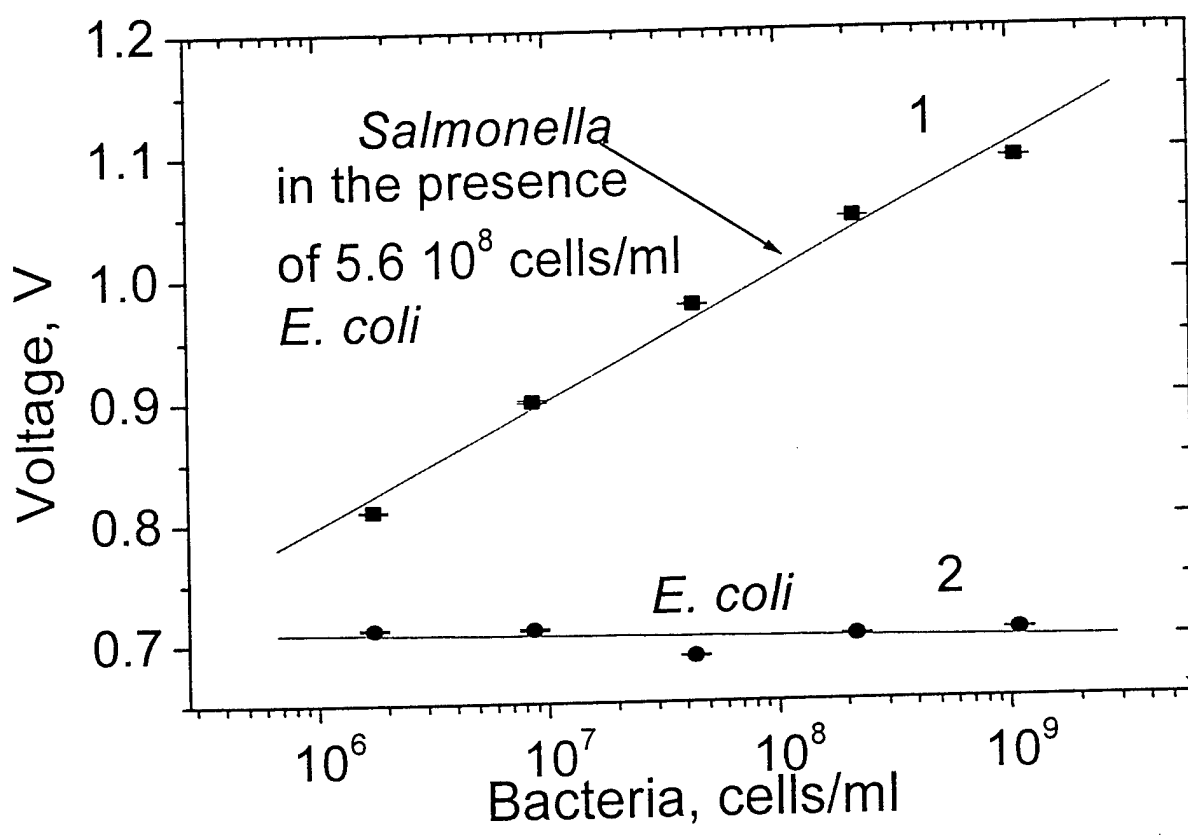


Figure 3



1 Figure 4



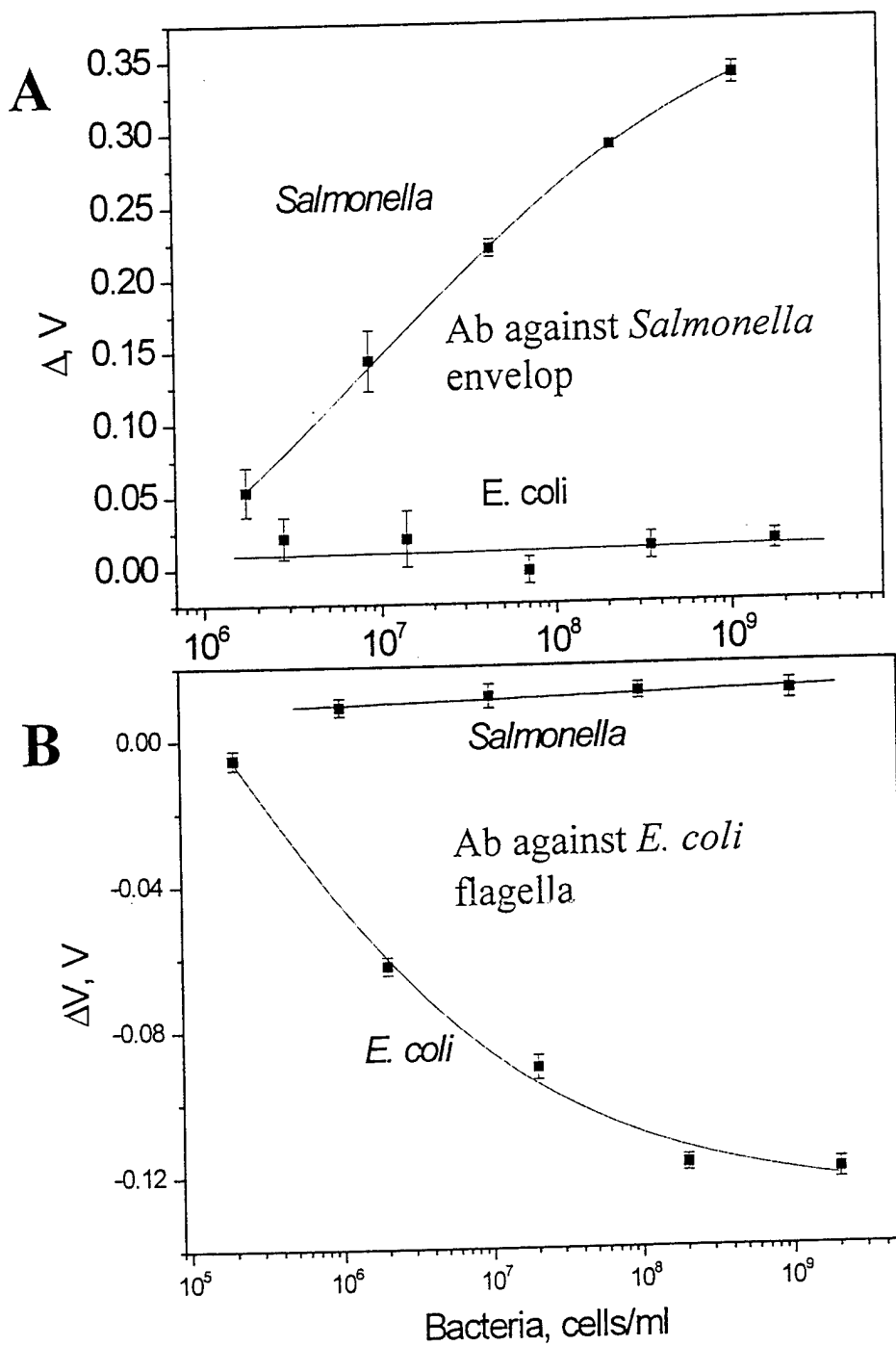
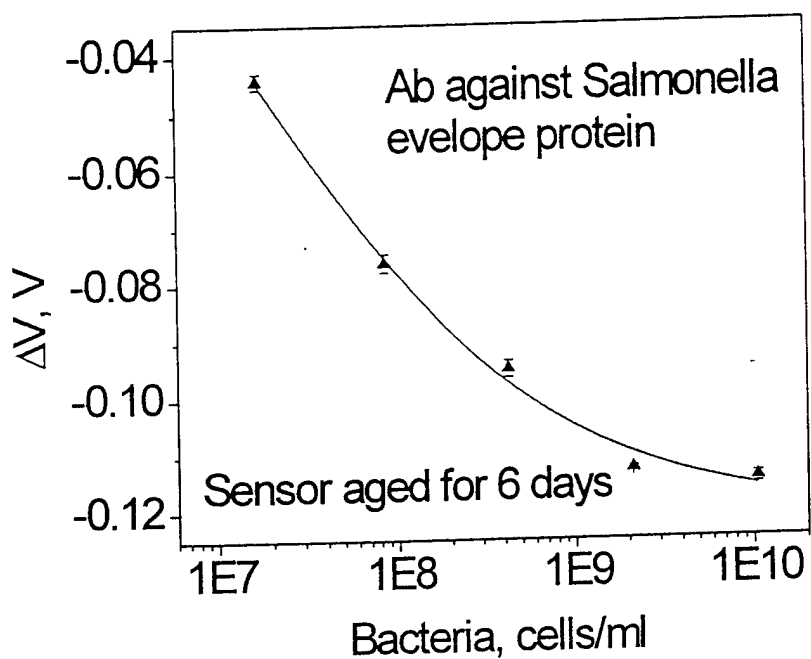
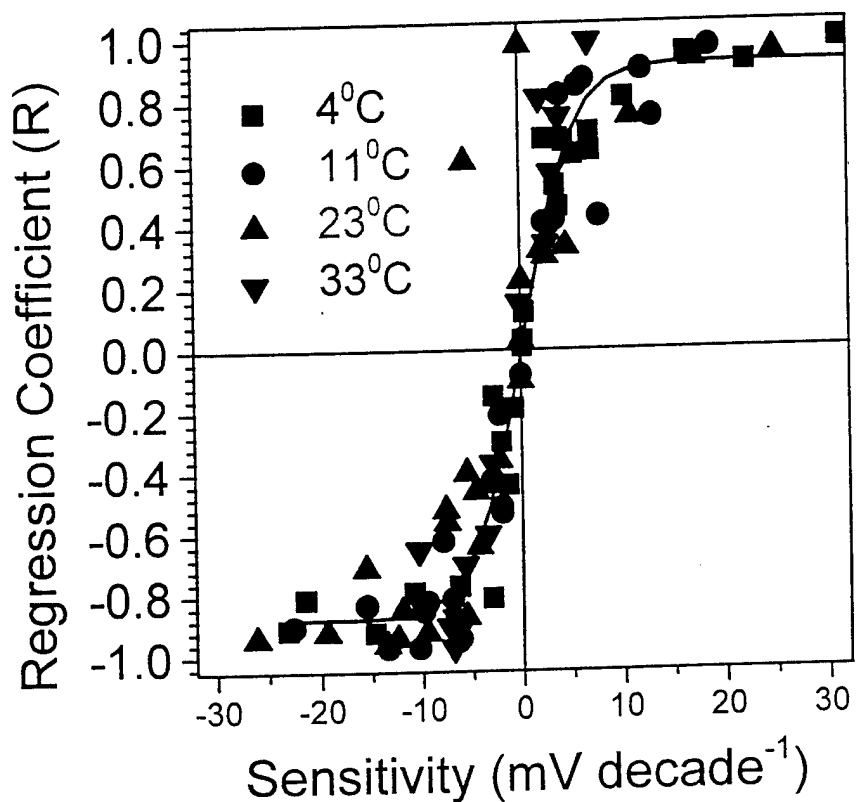


Figure 6

1
2



3
4 Figure 7
5
6



1
2 Figure 8
3

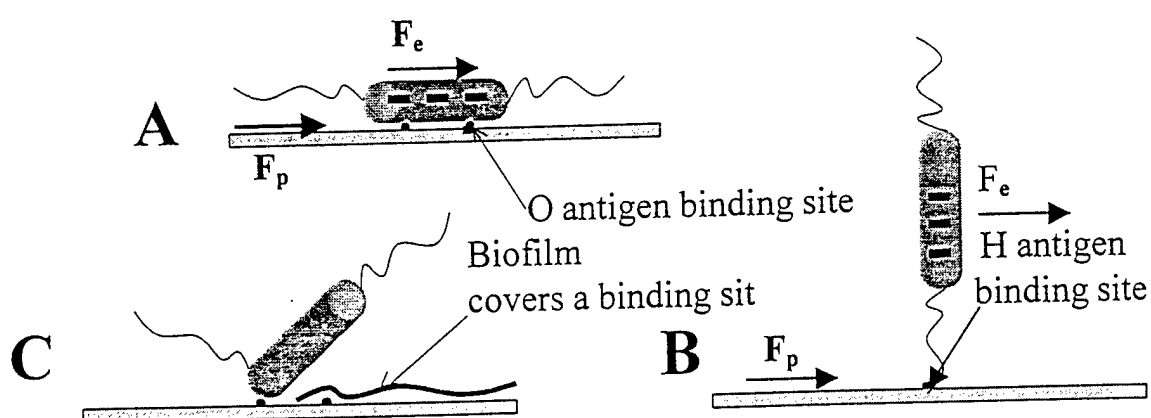


Figure 9

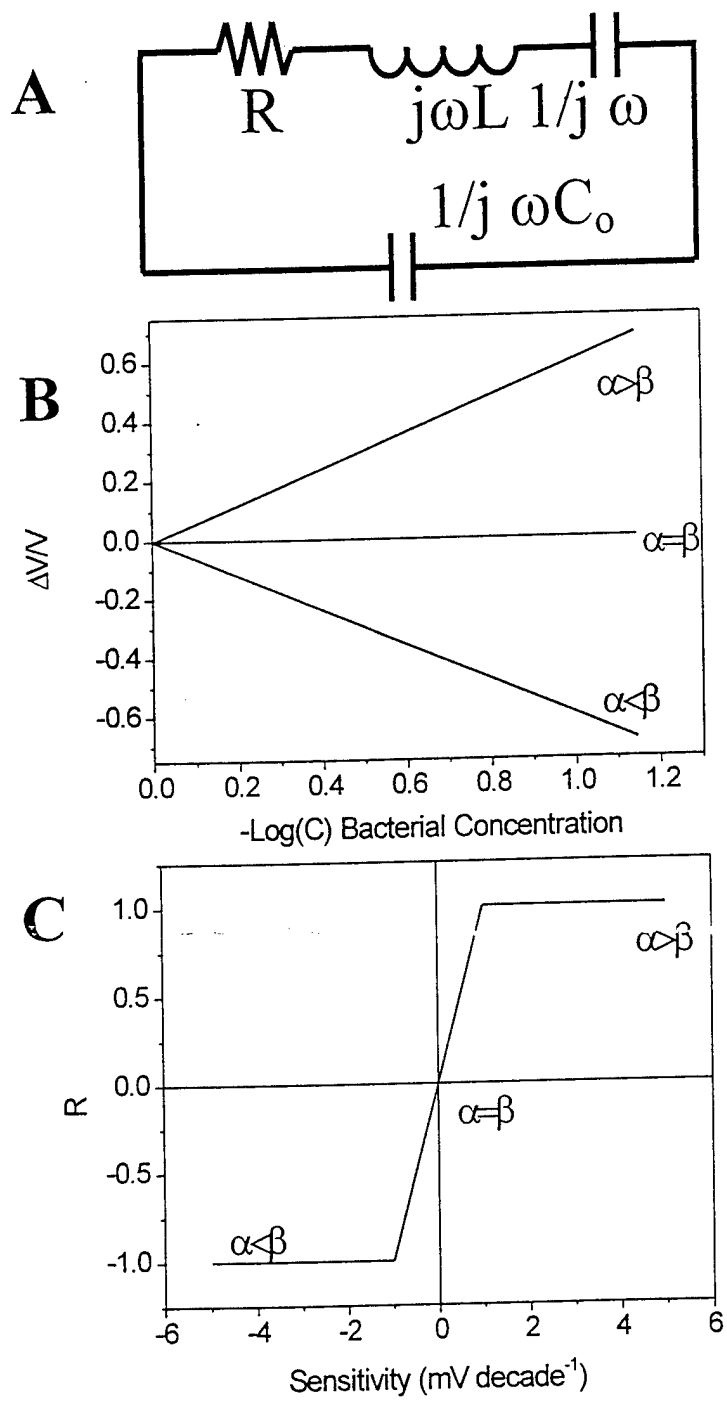


Figure 10.